Group. Balanced crystalloids versus saline in critically ill adults. *N Engl J Med* 2018;378:829–839.
3. Palevsky PM, Molitoris BA, Okusa MD, Levin A, Waikar SS, Wald R, *et al*. Design of clinical trials in acute kidney injury: report from an NIDDK workshop on trial methodology. *Clin J Am Soc Nephrol* 2012;7: 844–850.
4. McKown AC, Wang L, Wanderer JP, Ehrenfeld J, Rice TW, Bernard GR, *et al*. Predicting major adverse kidney events among critically ill adults using the electronic health record. *J Med Syst* 2017; 41:156.
5. Vincent J-L, Moreno R, Takala J, Willatts S, De Mendonça A, Bruining H, *et al*. The SOFA (Sepsis-related Organ Failure Assessment) score to describe organ dysfunction/failure. On behalf of the Working Group on Sepsis-Related Problems of the European Society of Intensive Care Medicine. *Intensive Care Med* 1996;22: 707–710.
6. Segal JB, Weiss C, Varadhan R. Understanding heterogeneity of treatment effects in pragmatic trials with an example of a large, simple trial of a drug treatment for osteoporosis. Center for Medical Technology Policy; 2011 [accessed 2018 Aug 10]. Available from: http://www.cmtpnet.org/docs/resources/Segal-Heterogeneity-in-Pragmatic-Trials.pdf.

Mycobacterial Lipids Induce Calcium Mobilization and Degranulation of Mast Cells

To the Editor:

Tuberculosis (TB) remains the leading cause of death from a single infectious agent, followed by HIV/AIDS (1). Emerging countries, such as Panama, have not been able to curb TB infection rates. The development of novel biomarkers for diagnosis, treatment monitoring, and vaccine development is urgently needed. The innate immune response during TB infection is a source of biomarkers. When a susceptible host is exposed to *Mycobacterium tuberculosis*, the bacteria translocate to the mucosal barrier, interacting with a variety of immune cells, including mast cells (MCs). The initial interaction between *M. tuberculosis* and first-line defense cells induces the accumulation and subsequent activation of these immune cells within lung tissue, and the release of proinflammatory mediators (2). Mycobacterial lipids appear to define the clinical fate of the infection by modulating the immune response during TB (3). However, the precise role of *M. tuberculosis* lipids in the immunopathogenic and molecular mechanisms of MC activation is still unknown.

MCs are abundant in the lung tissue, where they act as sentinels for a wide variety of invading pathogens, as well as regulatory cells during the course of acute inflammation (4). Besides specific antigen-driven IgE crosslink stimulation, MCs can be activated by complement components, IgG, neuropeptides, pathogen-associated molecular patterns, mainly peptides, and whole *M. tuberculosis* interaction (5). MC activation promotes the secretion of stored proinflammatory mediators as well as *de novo* synthesis of leukotrienes, platelet-activating factor, and prostaglandins. Together with the transcription and release of cytokines and chemokines by MCs, the host begins to make an adaptive immune response (6).

Recently, Garcia-Rodriguez and colleagues revised our perspective of the MC strategies used in bacterial defense and reported interactions occurring between *M. tuberculosis* and MCs (7). Shortly after exposure, MCs recognize *M. tuberculosis* via the TLR2 and CD48 receptors. During this initial stage, ESAT-6 and MPT-63 induce MC degranulation, cytokine release, and the secretion of antimicrobial peptides such as β-hexosaminidase and LL-37. We hypothesized that *M. tuberculosis* lipid extracts are able to activate MCs. In this preliminary study, we aimed to elucidate the role of single phospholipids and whole-lipid extracts in MC activation. Some results from these studies have been previously reported in the form of an abstract (8).

Methods

Cells and culture conditions. Murine MCs from line C1.MC/C57.1 (C57 MC) were kindly provided by Dr. Stephen Galli (Stanford University) and cultured in Dulbecco's modified Eagle's medium according to standard methods (9).

M. tuberculosis lipid extracts. The bacterial lipid fractions extracted from H37Rv *M. tuberculosis,* including total lipids (T-L, NR-14837), insoluble lipids (I-L, NR-14843), soluble lipids (S-L, NR-14842), *M. leprae*, phenolic glycolipid I (PGL-I, NR-19342), and *M. tuberculosis* phosphatidylinositol mannoside 6 (PIM6, NR-14847), were obtained from BEI Resources. Purified bovine heart L-α-phosphatidylcholine (PC, 840052C) and cardiolipin (CL, 840012C) were obtained from Avanti Polar Lipids. All *M. tuberculosis* lipid extracts were resuspended according to the manufacturer's recommendations.

β-Hexosaminidase release and calcium mobilization assays. C57 MCs were stimulated for 1 hour with T-L, S-L, I-L, PC, CL, PIM6, and PGL-I lipid fractions of *M. tuberculosis* at 20 μg/ml each. MC degranulation was determined by measuring β-hexosaminidase release according to a previously described protocol (10). Ionomycin was used as a positive control. Similarly, C57 MCs were stimulated with the above-mentioned lipids, and intracellular calcium levels were determined using a modified fluorimetric assay with Fluo 3-AM (Molecular Probes, Invitrogen) for intracellular calcium labeling (10). Student's *t* test was performed for all experiments, and *P* values of <0.05 were considered significant.

Results

M. tuberculosis lipid extract fractions significantly increased MC degranulation. β-Hexosaminidase release was measured to assess the degranulation capacity of C57 MCs after lipid

Supported in part by the National Secretariat of Science and Technology of Panama (SENACYT) through the Sistema Nacional de Investigadores and Programa Generación de Capacidades (APY-GC-2015-59) and Programa de Inserción de Talento Especializado (ITE-11-020 and ITE-11-018).

Author Contributions: Conception and design: I.T.-A. and A.G. Experiments, analysis, and interpretation: I.T.-A., A.G., S.R., C.O., and M.R. Drafting of the manuscript for important intellectual content: I.T.-A. and A.G.

Originally Published in Press as DOI: 10.1164/rccm.201803-0436LE on June 13, 2018

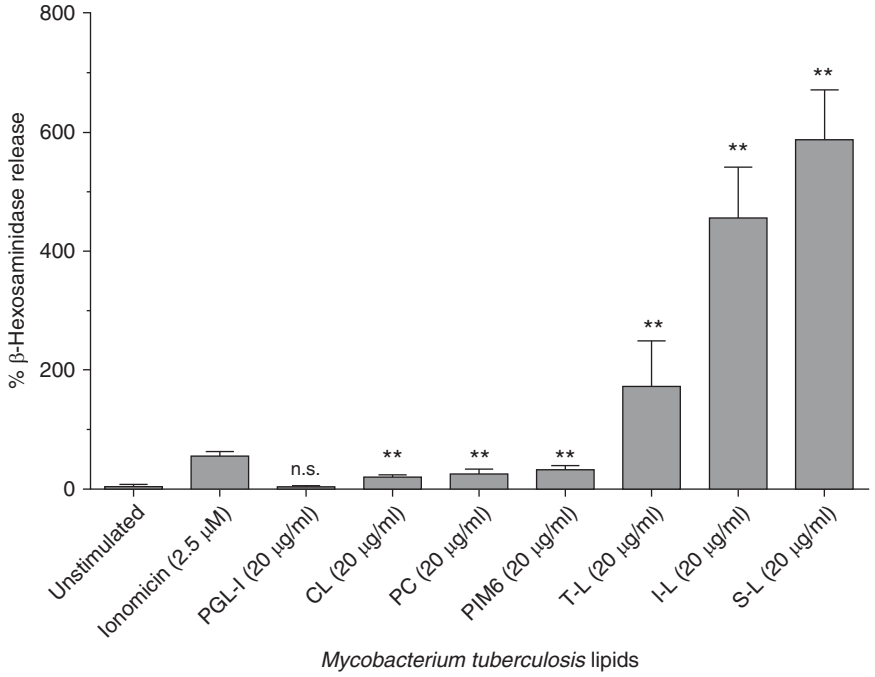

Figure 1. *Mycobacterium tuberculosis* lipid extract fractions stimulate C57 mast cell (MC) degranulation. C57 MCs were stimulated for 60 minutes with 20 μg/ml of total lipids (T-L), soluble lipids (S-L), insoluble lipids (I-L), phosphatidylcholine (PC), cardiolipin (CL), phosphatidylinositol mannoside 6 (PIM6), and phenolic glycolipid I (PGL-I) lipid extract fractions from *M. tuberculosis*. Ionomycin was used as a positive control. The I-L and S-L lipid extracts increased β-hexosaminidase release by 455.6% and 587.1%, respectively, which was significantly greater (**$P < 0.005$) than the increase observed with the ionomycin control (55.4%). In contrast, the stimulatory effects of the T-L, PC, CL, and PIM6 lipid extracts were considered to be significantly greater than those of the unstimulated control (**$P < 0.005$). The results are the average of three independent experiments. n.s. = not significant.

stimulation. The results indicated that all of the *M. tuberculosis* lipid extract fractions significantly increased ($P < 0.005$) β-hexosaminidase release compared with the unstimulated control, except for PGL-I. Only the I-L and S-L *M. tuberculosis* lipid extract fractions increased β-hexosaminidase release significantly more than the ionomycin control ($P < 0.005$) (Figure 1).

Soluble and insoluble M. tuberculosis lipid extract fractions induced high levels of calcium mobilization in MCs. MCs stimulated with 20 μg/ml of S-L and I-L *M. tuberculosis* lipid extract fractions showed the highest calcium mobilization levels (>15,000 relative fluorescence units) (Figure 2). Calcium mobilization in MCs was also higher in response to *M. tuberculosis* lipid extract fractions, including T-L, PIM6, and PGL-I, than in response to CL and PTC lipid extract fractions (Figure 2).

Discussion and Conclusions

Upon mucosal entry, bacteria and their lipid derivates interact with the first line of immune defenses. Here, we investigated the role of *M. tuberculosis* lipid extract fractions in MC activation. We observed that the C57 MCs responded to mycobacterial lipid extracts and were activated. We noted greater MC degranulation and increasing intracellular calcium mobilization in response to the S-L and I-L *M. tuberculosis* lipid extract mixtures compared with stimulation with the T-L fraction alone. A plausible explanation is that the *M. tuberculosis* S-L and I-L extract fractions contain a wide array of lipids with greater immunogenic properties than the T-L extract fraction stimuli. Also, the activation after stimulation with mycobacterial lipid extracts suggests that MCs respond specifically to *M. tuberculosis* lipids. A possible explanation is that TLR2 recognizes *M. tuberculosis* lipids. Further studies are warranted to describe the response of MCs to the whole *M. tuberculosis* bacterium interaction.

The mycobacterial cell envelope lipids constitute ~40% of the dry cell mass of *M. tuberculosis*. Their particular chemical structure, organization, and localization at the interface between the bacterium and the host play important roles in directing host–pathogen interactions. A small number of well-known *M. tuberculosis* antigens, such as ESAT-6, MTSA-10, and MPT-63, have been implicated in MC activation and mediator release (5). Our findings suggest that MCs have the potential to play an active role in mediating the innate host response to *M. tuberculosis*–derived lipid molecules. A better understanding of the interaction between MCs and *M. tuberculosis* lipids could lead to the development of new biomarkers, vaccines, or drugs against novel targets in *M. tuberculosis*. ■

Author disclosures are available with the text of this letter at www.atsjournals.org.

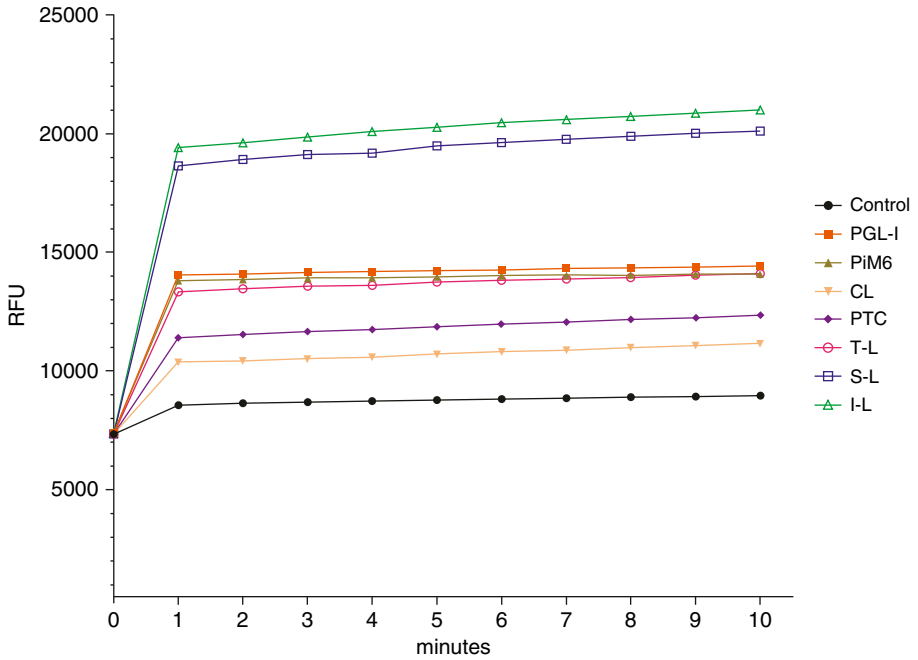

Figure 2. *Mycobacterium tuberculosis* lipid extract fractions induce C57 mast cell (MC) calcium mobilization. C57 MCs were stimulated for 60 minutes with 20 μg/ml of total lipids (T-L), soluble lipids (S-L), insoluble lipids (I-L), phosphatidylcholine (PTC), cardiolipin (CL), phosphatidylinositol mannoside 6 (PIM6), and phenolic glycolipid I (PGL-I) lipid extract fractions from *M. tuberculosis*. The results show calcium mobilization levels higher than 15,000 RFU after stimulation with I-L and S-L. The results are the average of three independent experiments. RFU = relative fluorescence units.

Acknowledgment: The authors thank Dr. Stephen Galli and Mindy Tsai from Stanford University for sharing the MC line C57 and providing training on laboratory techniques. They also thank BEI Resources for providing the *M. tuberculosis* lipid fractions, and Colleen Goodridge, Jordi Sintes Castro, Irene Oliver Vila, and Fernando de Mora for critically reviewing the manuscript.

Ivonne Torres-Atencio, M.Sc., Ph.D.
Universidad de Panamá
Panamá, Panama

and

Instituto de Investigaciones Científicas y Servicios de Alta Tecnología
Ciudad del Saber, Panama

Sara Rosero, B.S.
Ciara Ordoñez, B.S.
Instituto de Investigaciones Científicas y Servicios de Alta Tecnología
Ciudad del Saber, Panama

Michelle Ruiz, M.D.
Universidad de Panamá
Panamá, Panama

and

Instituto de Investigaciones Científicas y Servicios de Alta Tecnología
Ciudad del Saber, Panama

Amador Goodridge, M.Sc., Ph.D.
Instituto de Investigaciones Científicas y Servicios de Alta Tecnología
Ciudad del Saber, Panama

ORCID IDs: 0000-0001-5171-3439 (I.T.-A.); 0000-0003-3910-0482 (A.G.).

References

1. World Health Organization. Global Tuberculosis Report 2017 [accessed 2018 Jun 1]. Available from: http://www.who.int/tb/publications/global_report/en/.
2. Carlos D, de Souza Júnior DA, de Paula L, Jamur MC, Oliver C, Ramos SG, *et al*. Mast cells modulate pulmonary acute inflammation and host defense in a murine model of tuberculosis. *J Infect Dis* 2007;196: 1361–1368.
3. Queiroz A, Riley LW. Bacterial immunostat: *Mycobacterium tuberculosis* lipids and their role in the host immune response. *Rev Soc Bras Med Trop* 2017;50:9–18.
4. St John AL, Abraham SN. Innate immunity and its regulation by mast cells. *J Immunol* 2013;190:4458–4463.
5. Muñoz S, Rivas-Santiago B, Enciso JA. *Mycobacterium tuberculosis* entry into mast cells through cholesterol-rich membrane microdomains. *Scand J Immunol* 2009;70:256–263.
6. Galli SJ, Nakae S, Tsai M. Mast cells in the development of adaptive immune responses. *Nat Immunol* 2005;6:135–142.
7. Garcia-Rodriguez KM, Goenka A, Alonso-Rasgado MT, Hernández-Pando R, Bulfone-Paus S. The role of mast cells in tuberculosis: orchestrating innate immune crosstalk? *Front Immunol* 2017;8: 1290.
8. Rosero S, Torres I, Goodridge A. Mast cell C57 activation by *Mycobacterium tuberculosis* lipids and *Mycobacterium bovis* Bacille Calmette-Guerin (BCG) [abstract]. *Am J Respir Crit Care Med* 2016; 193:A5484.
9. Taylor AM, Galli SJ, Coleman JW. Stem-cell factor, the kit ligand, induces direct degranulation of rat peritoneal mast cells in vitro and in vivo: dependence of the in vitro effect on period of culture and comparisons of stem-cell factor with other mast cell-activating agents. *Immunology* 1995;86:427–433.

10. Torres-Atencio I, Ainsua-Enrich E, de Mora F, Picado C, Martín M. Prostaglandin E2 prevents hyperosmolar-induced human mast cell activation through prostanoid receptors EP2 and EP4. *PLoS One* 2014;9:e110870.

More on Single-Beat Estimation of Right Ventriculoarterial Coupling in Pulmonary Arterial Hypertension

To the Editor:

Right ventricular (RV) function is the main determinant of symptomatology and outcome in pulmonary arterial hypertension (PAH) (1). However, guidelines for the diagnosis and treatment of PAH do not advise on how best to measure RV function in these patients (2).

It has been better realized in recent years that RV adaptation in severe PAH is essentially homeometric, with an increase in contractility matching the increased afterload (1). As recently reviewed (3), the gold standard measure of RV contractility is end-systolic elastance (Ees), which is reasonably assumed equal to maximum elastance and defined by an end-systolic pressure (ESP) versus end-systolic volume relationship (1, 3). To assess the adequacy of RV contractility adaptation to afterload, Ees is expressed relative to arterial elastance (Ea), defined by an ESP versus stroke volume (SV) relationship (1, 3). The optimal coupling of the RV to afterload allowing for flow output at a minimal energy cost occurs at an Ees/Ea ratio of around 1.5 (3). When the Ees/Ea ratio decreases to 1 or below, the homeometric adaptation of the RV is exhausted. The RV then uses a dimensional or "heterometric" adaptation (Starling's law of the heart) to maintain flow output in response to metabolic demand (3).

Because of the major prognostic relevance of RV function, there is interest in an earlier and robust diagnosis of RV–arterial uncoupling and definition of critical Ees and Ees/Ea values associated with a risk for clinical deterioration. But how accurate are these measurements as currently performed in expert PAH centers?

Methods for assessment of RV–arterial coupling and their prognostic value were recently reviewed in detail by Tabima and colleagues (4). Ees can be measured from a family of pressure–volume loops at decreasing venous return (5) or by a single-beat method relying on the determination of a maximum pressure from nonlinear extrapolation of early and late isovolumic portions (before maximal and after minimal dP/dt, respectively) of the RV pressure curve (Figure 1) (6, 7). Ees is then equal to (maximum pressure − ESP)/SV, and Ea is equal to ESP/SV (3, 4).

Recent studies of RV–arterial coupling in severe PAH have assumed that mean pulmonary artery pressure (mPAP) would be an acceptable surrogate of ESP (3). However, this assumption is based on measurements in a small cohort of 15 patients, none of whom had PAH (five had pulmonary hypertension due to left heart disease), and with ESP measured at the PAP dicrotic notch (8). Although mPAP may be close to RV ESP in healthy individuals, the shape of RV pressure–volume loops in patients with severe PAH changes with increasing PAP, so that ESP becomes closer to RV systolic pressure than to mPAP (9).

In the present study, we quantified the error associated with Ees estimation using mPAP instead of ESP by measuring RV volumes and pressures with a conductance catheter (4F, CD Leycom) in 20 consecutive patients with PAH. The study was approved by the Institutional Review Board of the University of Giessen (#2015/108). All the patients gave written informed consent. There were 13 women and 7 men, aged 51 ± 15 years (mean ± SD). The diagnosis of PAH rested on a step-by-step approach to exclude pulmonary hypertension due to cardiac or pulmonary diseases and right heart catheterization showing mPAP >25 mm Hg and pulmonary vascular resistance >3 Wood units, in agreement with current recommendations (2). Results are expressed as mean ± SD when normally distributed (assessed by Kolmogorov-Smirnov test), and otherwise as median (interquartile range).

Seventeen patients had idiopathic PAH, one had portal hypertension–associated PAH, one had HIV-associated PAH, and one had systemic sclerosis–associated PAH. On the basis of hemodynamic measurements, pulmonary vascular resistance was 5.9 (interquartile range, 4.3–8.6) Wood units, mPAP was 41 ± 11 mm Hg, wedged PAP was 7 ± 2 mm Hg, and mixed venous oxygen saturation was 69 ± 6%. The patients were in New York Heart Association functional class III ($n = 12$) or II ($n = 8$).

As shown in Figure 1, there was a strong correlation between mPAP and ESP. The relationship between mPAP and ESP was described by a linear regression model as ESP = 1.65 × mPAP – 7.79 ($r = 0.932$; $r^2 = 0.868$; $P < 0.001$). However, this relationship differed from the line of identity with underestimation of ESP by mPAP in proportion to pulmonary hypertension severity. Pressure-dependent bias (indicating insufficient accuracy) and large limits of agreement (indicating insufficient precision) were confirmed on a Bland–Altman plot (10).

The comparison of Ees, Ea, and Ees/Ea calculated using mPAP versus ESP revealed significant differences (all $P < 0.001$, Wilcoxon signed rank test): Ees was calculated as 0.87 ± 0.44 versus 0.62 ± 0.38 mm Hg/ml (median difference, 0.18; range, 0.03–0.56), Ea was calculated as 0.52 ± 0.25 versus 0.76 ± 0.39 mm Hg/ml (median difference, −0.18; range, −0.56 to −0.02), and Ees/Ea was calculated as 1.84 ± 0.78 versus 0.89 ± 0.49 (median difference, 0.90; range, 0.20–1.85). These differences emphasize the importance of validating different contractility measurements.

Thus, mPAP cannot be a surrogate for RV ESP in the evaluation of RV contractility and RV–arterial coupling. Although the small sample size of our study must be considered, our results suggest that ESP can be cautiously estimated by the equation ESP = 1.65 × mPAP − 7.79 in the absence of direct measurements.

The study is funded by the German Research Foundation, Bonn, Germany (Collaborative Research Center 1213, "Pulmonary Hypertension and Cor Pulmonale" and Excellence Cluster "Cardio-Pulmonary System").

Author Contributions: K.T., M.J.R., W.S., H.A.G., and H.G. designed the study; K.T., M.J.R., J.A., and H.G. performed patient recruitment, care and follow-up; K.T., M.J.R., M.B., R.N., and H.G. performed data collection, maintenance, and analysis; M.J.R., J.A., M.B., W.S., R.N., H.A.G., and H.G. performed critical revision of the manuscript; and K.T. drafted the manuscript.

Originally Published in Press as DOI: 10.1164/rccm.201802-0283LE on May 14, 2018